

An Investigation into Panel Flutter with System Identification

Charles R. O'Neill*

Oklahoma State University, Stillwater, Oklahoma, 74078

CFD System identification was used to predict panel flutter for subsonic, supersonic and transonic flows. Finite element structural analysis determined the structural mode shapes and frequencies. A finite element flow solver determined the aerodynamic forces. The ARMA system identification process correctly identified the subsonic flutter boundary but failed for the supersonic and transonic cases.

Nomenclature

ARMA	Auto Regression Moving Average
STARS	STructural Analysis Routines
M	Mach number
ρ	Density, slugs/ft ³
$f(k)$	Force at step k
$q(k)$	Modal Displacement at step k
na	ARMA aerodynamic model order
nb	ARMA motion model order

Introduction

AEROELASTIC phenomenon enforce strict performance limits on aircraft. This study discusses aeroelastic prediction methods using system identification. The structural domain is a flexible panel with in-plane bending. Flutter boundaries for a specific panel will be found based on system identification. To check the boundary estimates, fully coupled unsteady cases will test and bound the actual flutter boundary.

Aeroelastic predictions require coupled aerodynamic and structural responses. This study first considers the structural aspects of the flexible panel. Next, the more difficult aerodynamics are discussed. The system identification process is discussed. Finally, aeroelastic predictions are made for a 1 by 2 foot panel at Mach 0.5, 0.95 and 3.0.

Structural Analysis

Aeroelasticity requires a flexible body. A three dimensional aluminum plate will be used for all structural properties. The plate's edges are clamped for no rotation or displacement. Table 1 gives the sizing and material properties of the plate. It is noted that the thickness, 0.1 inches, is significantly thicker than most aircraft skins.

STARS Solids, a finite element structural solver developed at NASA Dryden¹, was used to calculate the free vibration mode shapes and frequencies. First, a finite element structural grid was created. A 512 element structural grid gave sufficiently smooth mode shapes and is shown in Fig. 1.

Next, the STARS Solids program was run. All computations were started through the `cfdsaserun` utility shell. The `stars.bat` GUI interface is also available. Total solution time is on the order of 5 seconds for the 512 element grid on an Athlon XP 1800. Hindsight revealed that a finer structural grid would be worth the small increase in Solids computational time.

Mode shapes from STARS Solids were interpolated to the CFD mesh using `cfdsaserun`. All modes are scaled to the same maximum deflection. Mode shapes and frequencies for the plate are shown in Fig 2. The first four modes oscillate lengthwise with node lines widthwise. The fifth and sixth oscillate across their width with lengthwise node lines.

*Graduate Research Assistant, Mechanical and Aerospace Engineering. Student Member AIAA.

Presented at the MAE 5933 Project Presentations, 9 May 2002. Copyright © 2002 by Charles R. O'Neill. Published by the American Institute of Aeronautics and Astronautics, Inc. with permission.

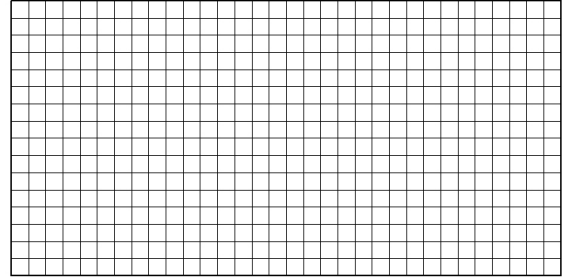


Fig. 1 Structural Grid (32 x 16)

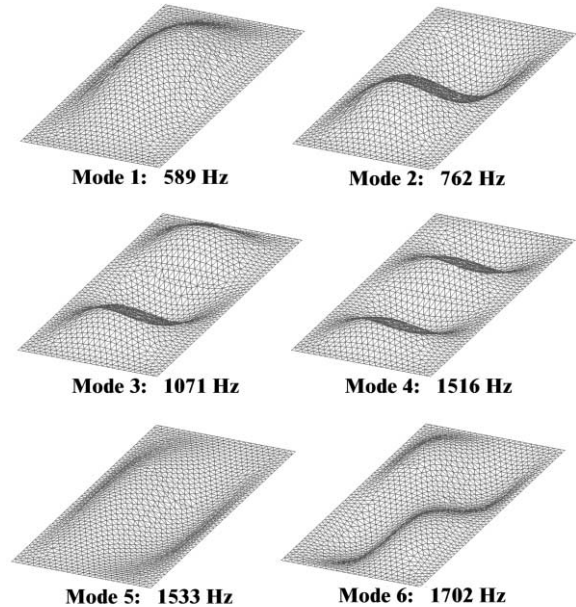


Fig. 2 Mode Shapes and Frequencies

The fourth and fifth modes have approximately the same frequency (1500 Hz).

Modal mass, stiffness and damping matrices were created from the Solids .out files. The `cfdsaserun` utility automatically created the .arrays modal matrices file. Solids does have one subtle problem. The Solids program often exports shifted modal mass and stiffness matrices. If the eigen-

Table 1 Aluminum Plate Properties

Plate Properties	
Length	2 ft
Width	1 ft
Thickness	0.10 in
Density	0.4458 slugs/ft ³
Elastic Modulus	10.0 · 10 ⁶ psi

value shifting occurs, a FMM scaling factor is included with the `genmass` output. If FMM is non-zero, the `massshift3d` utility must be run to shift the modal matrices to the `euler3d` format. Original STARS `unsteady` correctly interprets FMM; `euler3d` does not. Unfortunately, the `cfdaserverun` does not pass the FMM parameter through, so manual intervention is *always* needed if FMM is non-zero.

Aerodynamics Analysis

Aeroelasticity also requires aerodynamic forces. The fluid flow domain is based on the structural panel geometry. Curves and surfaces were created to define the appropriate interface between the structural model and the fluid geometry. The final finite element grid consists of 14000 surface elements and 283654 elements in the entire three dimensional domain. Fig 3 shows the finite element grid for the flexible plate and the surrounding in-plane wall. The flow domain extends 1 foot from the flexible plate's side and 2 feet from each of the plate's ends. Fluid enters on the left

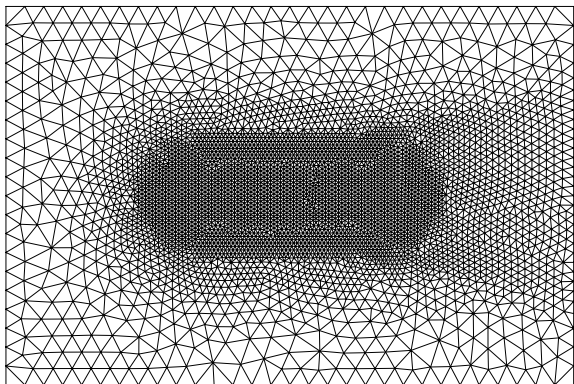


Fig. 3 Finite Element Grid

and exits on the right. The flexible panel is located in the center of the bottom wall. A finer grid spacing is specified near the flexible plate to catch any high gradients. The fine spacing aft (right) of the panel captures any wakes or shocks emanating from the panel.

Finite Element CFD solver

A finite element three-dimensional transient flow solver was used for all computations. This `euler3d` program was developed in the OSU CASELab for aeroelastic predictions. The `euler3d` program solves the well-known Euler equations for inviscid flow with artificial dissipation added for solution stability. Unsteady fluid motion is determined through with local flow property iterations within a global time-march procedure.

Structural mode shapes are coupled with the fluid flow in `euler3d` with transpiration which is an appropriate modification of surface normals. For small deflections, transpiration properly changes the surface boundary conditions without remeshing the domain.

System Identification

For this study, system identification focuses on determining a linear model for the aerodynamics about an operating point. Combining this linear aerodynamics model with a linear structural model allows for simple and rapid aeroelastic predictions. Cowan² developed a system identification routine for STARS and `euler3d`.

Theory

System identification reduces to a simple foundation. If an system's input and output are known, we can determine a model for that system. A perfect model would perfectly mimic the original system.

The CASELab's system identification method consists of forming an ARMA model from motion inputs and aerodynamic force outputs. The current aerodynamic forces

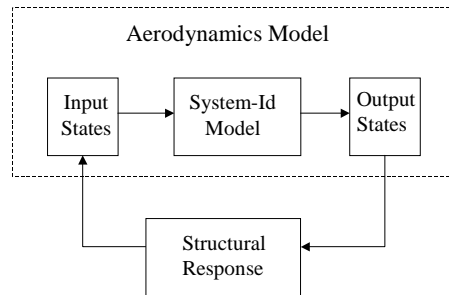


Fig. 4 System Identification Flow Diagram

depend on previous forces and motions.

$$f_a(k) = \sum_{i=1}^{na} [A] f_a(k-i) + \sum_{i=1}^{nb-1} [B] q(k-i)$$

The ARMA model picks values for $[A]$ and $[B]$ that provide the best fit between the input and output. Once an ARMA model is created, the aerodynamics and structures are coupled to form a state space representation of the entire aeroelastic system. Fig 4 shows a schematic state flow diagram for the coupled system. For aeroelastic predictions, the primary focus is coupled stability. Since the coupled aeroelastic state space form is known, the stability criteria reduces to determining eigenvalues.

Multistep

Since the ARMA model relies on input, a successful training signal must sufficiently excite any frequencies wanted in the output. A training signal lacking a particular frequency will prevent the ARMA routine properly predicting that frequency. The current training signal is a variable amplitude multistep (VAMS). The VAMS is based on a 7-5-3-2-1-1 multistep. To maintain a constant maximum displacement, each step velocity is varied. Fig 5 shows the velocity, displacement and power spectral densities for the variable amplitude multistep. The multistep's power level

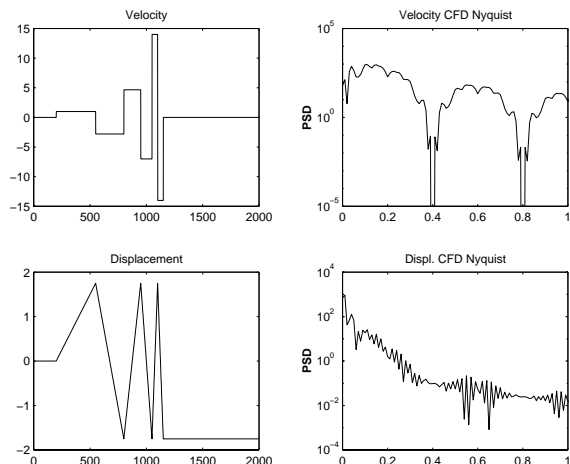


Fig. 5 Variable Amplitude Multistep PSD

drops for displacement frequencies below 40 percent of the CFD Nyquist frequency. Dead frequencies are unwanted, thus we are restricted to a certain frequency bandwidth. This restriction is not as problematic as it appears; the CFD solver typically needs at least 30 steps per cycle of the highest frequency for an accurate time-marched solution.

The CFD and ARMA time scales must be compatible with the problem's physical time scale. CFD requires small time steps for proper time-marching. Physics requires a sufficiently long excitation and observation window. To be effective, the ARMA routine must satisfy the physics while starting from a CFD solution. Fig 6 shows the relationship between CFD, ARMA and physical time scales.

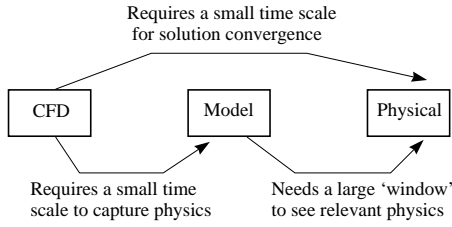


Fig. 6 Time Scale

Results

Aeroelastic predictions were performed at three Mach numbers: 0.5, 0.95 and 3.0. For each Mach number, an ARMA model prediction is made. Actual free response runs are then compared to the ARMA model's prediction. Computations were performed on 4 machines: a 500MHz Alpha 21264, an 800MHz Athlon, a 1000MHz Athlon and an XP 1800 Athlon. The entire study exclusively used Euler3d version 2.11 which includes the new first order force integration routine.

Mach 0.5

A subsonic test at Mach 0.5 was performed. An ARMA analysis determined a flutter boundary. Free response runs were used to bound the ARMA boundary.

ARMA

A variable amplitude multistep was used to train the ARMA model. The multistep had an amplitude of 0.1 and an isize of 7. This isize corresponds to one-half wavelength of the lowest frequency for the multistep's 7 step.

Initial experimentation did not reveal a converging flutter boundary. Thus, a model sensitivity study was used to sweep over multiple model orders. Fig 7 shows the dynamic flutter boundary for dynamic pressure over a range of nb terms. The na terms are plotted as different lines. The only converged boundary exists for na between 15 and 30.

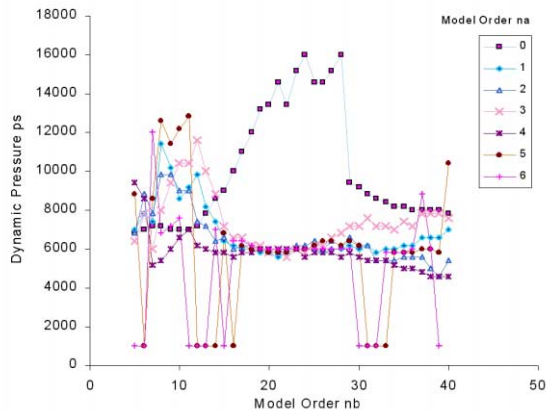


Fig. 7 Model Sensitivity (M=0.5)

To further investigate this converged area, the eigenvalues were calculated for a 5-20 model order. Fig 8 shows the structural modes 1 through 6 as a function of dynamic pressure. Mode 3 exits the unit circle first at 5900 psf. For the converged flutter boundaries in Fig 7, mode 3 diverges at approximately 6000 psf. With reasonable certainty, the Mach 0.5 panel flutter occurs at 6000 psf (0.04 slugs/ft³).

Unsteady Euler3d

Unsteady euler3d simulations provide an accurate aerostructural time history. Successive iterations were used to bound the flutter point. Fig 9 shows a modal time history at a density of 0.02 slugs per ft³ (3000 psf). The time history clearly shows a damped response for all modes and forces.

Fig 10 shows the time history for a density of 0.05 slugs per ft³ (6800 psf). The displacements are undamped or per-

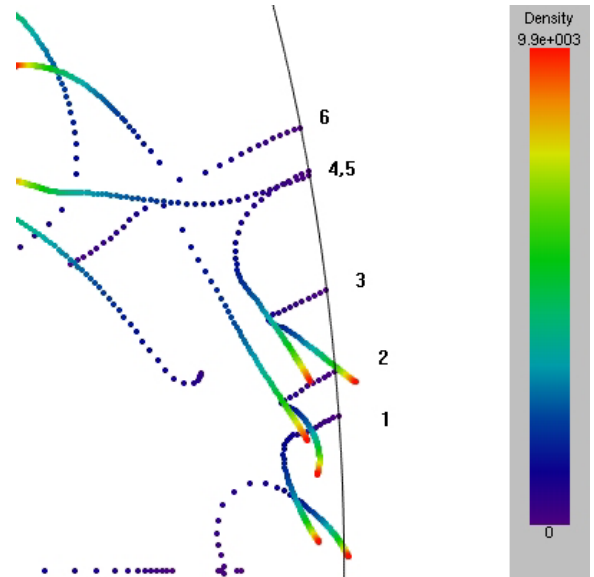
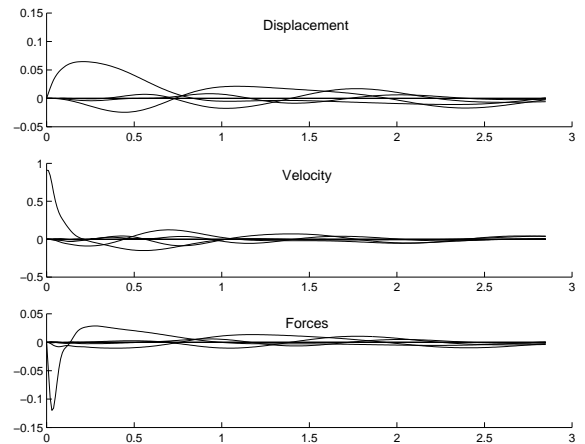
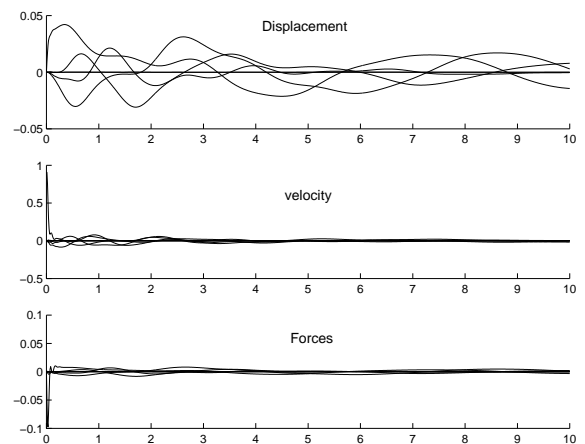


Fig. 8 Eigenvalues 5-20 Model (M=0.5)

Fig. 9 Time History $\rho = 0.02$ (M=0.5)Fig. 10 Time History $\rho = 0.05$ (M=0.5)

haps slightly damped. The theval time history evaluator gives a damping ratio of zero for the first 5 modes. Thus, the flutter boundary at Mach 0.5 appears to be approximately 7500 psf (0.05 slugs/ft³). However, the exact neutral point is difficult to find and would take significantly more computational power.

A third modal time history is shown in Fig 11 for a density of 0.1 slugs per ft³ (15000 psf). The time history for mode 3 dynamically diverges. Interestingly, mode 2 statically con-

verges to -0.25. From the eigenvalue plot, it appears that mode 1 is heading towards zero frequency. This matches the linear subsonic 2D panel flutter theory's prediction of first mode divergence.

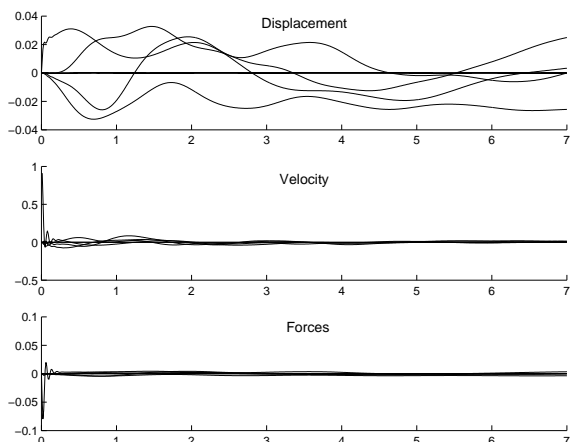


Fig. 11 Time History $\rho = 0.1$ ($M=0.5$)

The free response trials suggest that the ARMA estimate of 6000 psf is slightly low. An unknown factor apparently causes the ARMA model to fail for model orders outside a specific range. Other testcases have exhibited ARMA model divergence for large model orders; however, this testcase has one of the worst "prediction ranges" known so far! Overall, the ARMA found a conservative flutter boundary within a margin of approximately 10 to 15 percent of the actual boundary.

Mach 3.0

The same testcase was run at Mach 3.0. A similar procedure was used to find an ARMA flutter boundary. Again, free response runs were made to find the flutter boundary. Because this flow is supersonic, the piston perturbation method is available.

ARMA

An ARMA based variable amplitude multistep was run for the geometry at Mach 3.0. The multistep had an amplitude of 0.1 and an isize of 8.

A model sensitivity study gave badly variable results for all model orders other than $na=0$. Fig 12 shows the embarrassingly awful model sensitivity study. All model orders

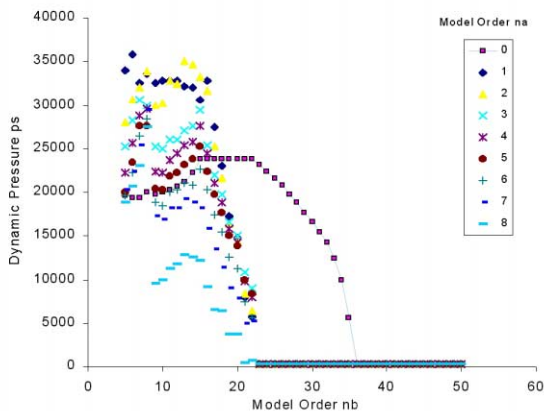


Fig. 12 Model Sensitivity ($M=3.0$)

tend towards a flutter boundary of zero dynamic pressure for any nb order over 20. Unlike the Mach 0.5 case, there are no concurrent similar estimates between the models. The most consistent ARMA predictions occurred with $na=0$ and nb around 20. For a 0-20 model, the ARMA model predicts a mode 1 dynamic divergence at 23800 psf ($0.00437 \text{ slugs/ft}^3$)

Piston

Next, a free response piston perturbation method determined the Mach 3.0 flutter boundary. The piston response for a free stream density of 0.004 slugs/ft^3 (2200 psf) yields Fig 13 which is clearly stable. The free-stream density was

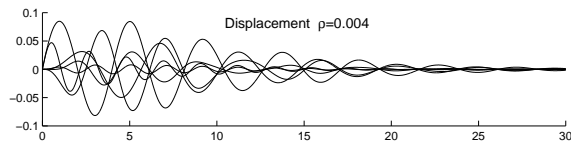


Fig. 13 Time History $\rho = 0.004$ ($M=3.0$)

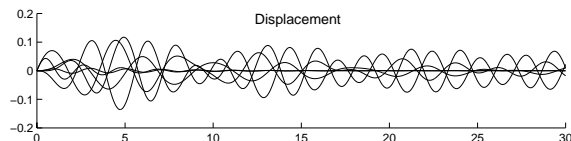


Fig. 14 Time History $\rho = 0.008$ ($M=3.0$)

increased until a the piston method predicted a neutral response. Fig 14 shows the neutrally stable response at a density of 0.008 slugs/ft^3 . The piston perturbation method determined a flutter boundary two times higher than the ARMA model!

Unsteady Euler3d

The unsteady euler3d program tested for flutter in the ARMA and piston prediction range. The first run was just below the ARMA flutter prediction. Fig. 15 shows the time history at $\rho = 0.004$. The solution is damped. Next, an

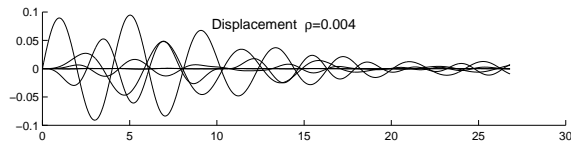


Fig. 15 Time History $\rho = 0.004$ ($M=3.0$)

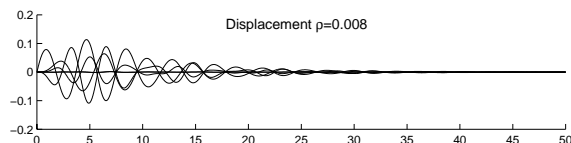


Fig. 16 Time History $\rho = 0.008$ ($M=3.0$)

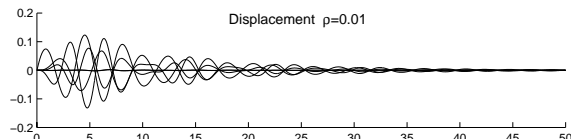


Fig. 17 Time History $\rho = 0.01$ ($M=3.0$)

unsteady euler3d free response was run at the piston flutter boundary. Fig. 16 shows the time history at $\rho = 0.008$. Again, the solution is damped.

As a final test, a free stream density of 0.01 slugs/ft^3 was tested. Again the response is damped. Fig. 17 shows the time history at $\rho = 0.01$.

Both the ARMA and piston methods failed to find the true Mach 3 flutter boundary. At 2.5 times the ARMA prediction, an euler3d free response is still clearly damped.

Mach 0.95

A testcase at Mach 0.95 allows for challenging transonic flow. To check for shocks, a steady case was run a steady panel deflection. Next, an ARMA model predicted the flutter boundary. Finally, coupled unsteady responses tested the ARMA's boundary.

Steady State

A steady state Mach 0.95 case was solved to show the transonic nature of the flow. The solution was run to convergence for a 2nd mode deflection of 0.2 units. Fig 18 shows the mach distribution along the plate and surrounding wall.

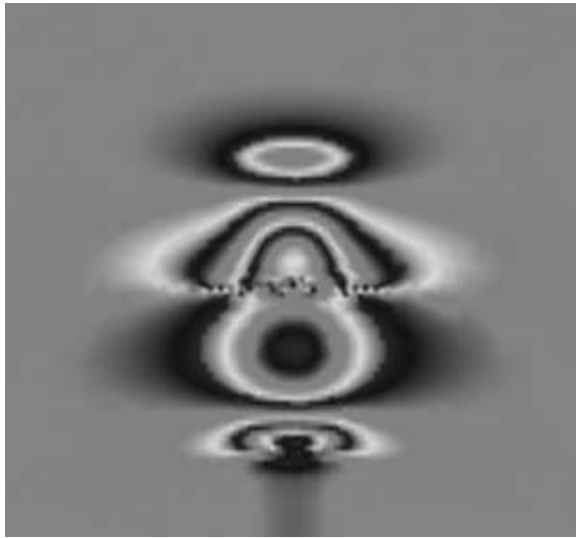


Fig. 18 Mach Distribution (M=0.95)

The flow accelerates to supersonic over the first portion of the plate. A shock occurs after the first geometrical peak. Afterwards, the flow accelerates to supersonic again at the second peak. Fig 19 shows a cross sectional cut of Mach number along the plate centerline. The geometry's vertical axis is enlarged by 4 times. Clearly, this transonic testcase will challenge any attempt at system identification with flow non linearities and discontinuities.

ARMA

An ARMA based variable amplitude multistep was run for the geometry at Mach 0.95. Fig 20 shows a model sensitivity study. The ARMA flutter estimates appear to converge to 13000 psf (0.0238 slugs/ft³).

Unsteady Euler3d

Three unsteady euler3d time responses were run to check the ARMA prediction and establish a true boundary. At the ARMA prediction of $\rho = 0.0237$, Fig. 21 shows the damped time response. Because the ARMA solution clearly failed, determining the approximate boundary through free response iterations was attempted. Fig. 22 shows a near neutral stability free response at $\rho = 0.05$. This is twice the ARMA model's prediction. Fig. 23 shows a divergent

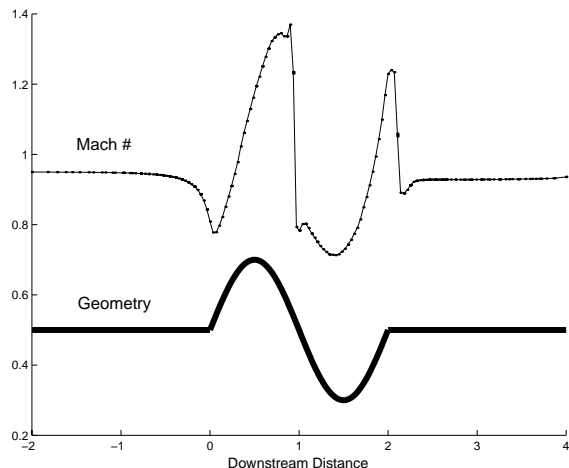


Fig. 19 Streamwise Cut (M=0.95)

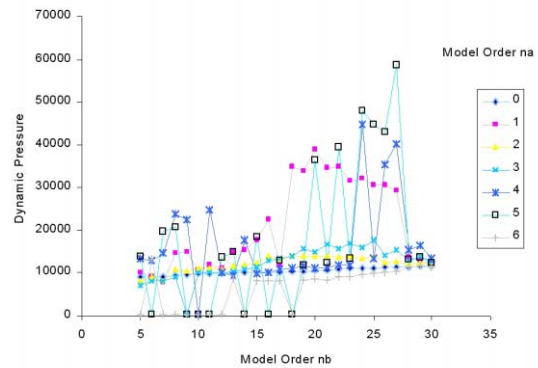


Fig. 20 Model Sensitivity (M=0.95)

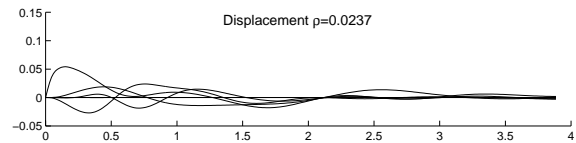


Fig. 21 Time History $\rho = 0.0237$ (M=0.95)

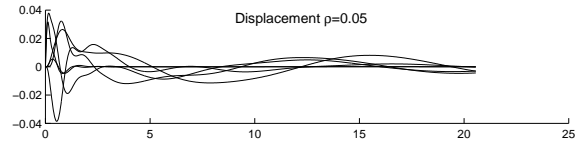


Fig. 22 Time History $\rho = 0.05$ (M=0.95)

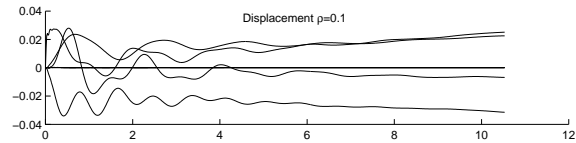


Fig. 23 Time History $\rho = 0.1$ (M=0.95)

time response at $\rho = 0.1$.

The ARMA model failed for the transonic Mach 0.95 test-case. A model sensitivity study shows the wildly variable ARMA predictions. The free response boundary is approximately twice higher than the ARMA prediction.

Conclusions

A panel flutter testcase was investigated. The STARS structural analysis package was integrated with the euler3d CFD solver for a 6 mode panel flutter testcase. The cfdaserun and makevec3d utilities now correctly converts modal matrices and mode shapes between STARS Solids output and euler3d vector files.

The ARMA system identification theory is reviewed. The ARMA routine is theoretically useful regardless of the aerodynamic solution method.

Panel flutter was investigated at three Mach numbers: 0.5, 0.95, and 3.0. Only the Mach 0.5 example had a clear and converged ARMA prediction. The Mach 0.5 ARMA prediction appears to be within 10 to 15 percent of the correct boundary. The ARMA predictions at Mach 3.0 and 0.95 failed. For these Mach numbers, the model sensitivity analysis shows little convergence for any model order.

References

¹Gupta, K. K., "STARS—An Integrated Multidisciplinary, Finite-Element, Structural, Fluids, Aeroelastic and Aerosevaelastic Analysis Computer Program," NASA-TM-4795, April 2001.

²Cowan, T. J., Arena, A. S., and Gupta, K. K., "Accelerating Computational Fluid Dynamics Based on Aeroelastic Predictions Using System Identification," *Journal of Aircraft*, Vol. 38, No. 1, January-February 2001, pp. 81-87.